CANADIAN APPLIED
MATHEMATICS QUARTERLY
Volume 19, Number 3, Fall 2011

MODELING CHOLERA DYNAMICS WITH CONTROLS

JIN WANG AND CHAIRAT MODNAK

ABSTRACT. In this paper, we present and analyze a cholera epidemiological model with control measures incorporated. This model is extended from the one proposed in [**16**] by including the effects of vaccination, therapeutic treatment, and water sanitation. Equilibrium analysis is conducted in the case with constant controls for both epidemic and endemic dynamics. Optimal control theory is applied to seek cost-effective solution of multiple time-dependent intervention strategies against cholera outbreaks.

1 Introduction Cholera is an acute intestinal infectious disease caused by the bacterium *Vibrio cholerae*. Recent cholera outbreaks in Haiti (2010–2011), Nigeria (2010), Kenya (2010), Vietnam (2009), Zimbabwe (2008–2009), etc., continue leading to a large number of infections and receiving worldwide attention [**5, 26**].

The dynamics of cholera involve multiple interactions between the human host, the pathogen, and the environment [**18**], which contribute to both direct human-to-human and indirect environment-to-human transmission pathways. In an effort to gain deeper understanding of the complex dynamics of cholera, several mathematical models have been published. For example, Codeço in 2001 proposed a model [**6**] that explicitly accounted for the environmental component, i.e., the *V. cholerae* concentration in the water supply, into a regular SIR epidemiological model. The incidence (or, the infection force) was modeled by a logistic function to represent the saturation effect. Hartley, Morris and Smith [**9**] in 2006 extended Codeço's work to include a hyperinfectious state of the pathogen, representing the "explosive" infectivity of freshly shed *V. cholerae*, based on the laboratory observations [**1, 15**]. This model was rigorously analyzed in [**14**]. Joh, Wang, Weiss *et al.* [**11**] in 2009 Modified Codeço's model by a threshold pathogen density for infection,

Keywords: Cholera, dynamical systems, stability, optimal control.

with a careful discussion on human-environment contact and in-reservoir pathogen dynamics. More recently, Mukandavire *et al.* [**16**] proposed a model to study the 2008–2009 cholera outbreak in Zimbabwe. The model explicitly considered both human-to-human and environment-to-human transmission pathways. The results in this work demonstrated the importance of the human-to-human transmission in cholera epidemics, especially in such places as Zimbabwe, a land-locked country in the middle of Africa. Moreover, Tien and Earn [**24**] in 2010 published a water-borne disease model which also included the dual transmission pathways, with bilinear incidence rates employed for both the environment-to-human and human-to-human infection routes. No saturation effect was considered in Tien and Earn's work. A rigorous global stability analysis was conducted in [**23**] for many of the afore-mentioned models. In addition, Neilan *et al.* [**17**] in 2010 modified the cholera model proposed by Hartley, Morris and Smith [**9**] and added several control measures into the model. They consequently analyzed the optimal intervention strategies and conducted numerical simulation based on their model. No human-to-human infection route is considered in this work.

In the present paper, we aim to better understand the effects of different control measures coupled with multiple transmission pathways of cholera, so as to gain useful guidelines to the effective prevention and intervention strategies against cholera epidemics. To that end, we study cholera dynamics with control measures incorporated into the model of Mukandavire *et al.* [**16**] which involve both the environment-to-human and human-to-human transmission modes. We modify the original model by adding three types of controls: vaccination, therapeutic treatment (including hydration therapy, antibiotics, etc.), and water sanitation. In general, these control measures are functions of time. For the special case with constant controls, we are able to rigorously analyze the stabilities of the corresponding autonomous dynamical system. For time-dependent controls, we will examine how the effects and costs of control measures can be best balanced. Specifically, we will formulate a state-adjoint system and derive the necessary conditions for the optimal control strategies. We will then use numerical simulation to explore various optimal control solutions involving single and multiple controls.

In what follows, we will first present the cholera model with control measures incorporated. We will next conduct an equilibrium analysis for the epidemic and endemic dynamics of the system when the rates of the controls are constant. Then we will turn to the time-dependent control system and perform an optimal control study for the cholera model. Finally we will draw conclusions to close the paper.

2 Mathematical model Let $S(t)$, $I(t)$ and $R(t)$ denote the susceptible, the infected, and the recovered human population sets, respectively. The total population $N = S + I + R$ is assumed to be a constant, which is a reasonable assumption for a relatively short period of time and for low-mortality diseases such as cholera. Let also B denote the concentration of the vibrios in the environment (e.g., contaminated water). The cholera model developed in [**16**] is a combined system of human populations and the environmental component (SIR-B), with the environment-to-human transmission represented by a logistic (or, Michaelis-Menten type) function and the human-to-human transmission by the standard mass action law.

We now extend this model by adding vaccination, treatment and water sanitation. We assume these controls are implemented continuously; specifically, we make the following assumptions:

- Vaccination is introduced to the susceptible population at a rate of $v(t)$, so that $v(t)S(t)$ individuals per time are removed from the susceptible class and added to the recovered class.
- Therapeutic treatment is applied to the infected people at a rate of $a(t)$, so that $a(t)I(t)$ individuals per time are removed from the infected class and added to the recovered class.
- Water sanitation leads to the death of vibrios at a rate of $w(t)$.

As a result, we obtain the following dynamical system:

$$\frac{dS}{dt} = \mu N - \beta_e S\frac{B}{\kappa + B} - \beta_h SI - \mu S - v(t)S, \tag{1}$$

$$\frac{dI}{dt} = \beta_e S\frac{B}{\kappa + B} + \beta_h SI - (\gamma + \mu)I - a(t)I, \tag{2}$$

$$\frac{dB}{dt} = \xi I - \delta B - w(t)B. \tag{3}$$

In addition, we have the equation for R:

$$\frac{dR}{dt} = \gamma I - \mu R + a(t)I + v(t)S, \tag{4}$$

though this equation is not needed in the model analysis since $R = N - S - I$. In this system, the parameter μ, ξ, δ, γ, κ, β_e and β_h are all positive constants; μ denotes the natural human birth/death rate, ξ is the rate of human contribution (e.g., shedding) to *V. cholerae*, δ is the natural death rate of *V. cholerae*, γ is the rate of recovery

from cholera, κ is the pathogen concentration that yields 50% chance of catching cholera, and β_e and β_h represent rates of ingesting vibrios from the contaminated water and through human-to-human interaction, respectively. A typical set of numerical values for these parameters are listed in Table 1 (see Section 4). In particular, when all controls are set to zero, i.e., $v = a = w = 0$, the above system is reduced to the original model developed in [**16**].

3 Equilibrium analysis For the special case when the rates of all the three controls are positive constants, i.e., $v(t) = v > 0$, $a(t) = a > 0$, and $w(t) = w > 0$, the model (1–3) is reduced to an autonomous system

$$\frac{dS}{dt} = \mu N - \beta_e S \frac{B}{\kappa + B} - \beta_h SI - \mu S - vS, \tag{5}$$

$$\frac{dI}{dt} = \beta_e S \frac{B}{\kappa + B} + \beta_h SI - (\gamma + \mu)I - aI, \tag{6}$$

$$\frac{dB}{dt} = \xi I - \delta B - wB. \tag{7}$$

This allows us to conduct a careful equilibrium analysis to investigate the effects of controls on the epidemic and endemic dynamics of cholera.

3.1 Epidemic dynamics The disease-free equilibrium (DFE) for the model (5–7) is given by

$$\mathcal{E}_0 = \left(\frac{\mu N}{\mu + v}, 0, 0 \right). \tag{8}$$

We first compute the basic reproductive number for this model using the method of van den Driessche and Watmough [**25**]. Here, the associated next generation matrices are given by

$$F = \begin{bmatrix} \mu\beta_h \frac{N}{\mu+v} & \frac{\mu\beta_e}{\kappa}\frac{N}{\mu+v} \\ 0 & 0 \end{bmatrix} \quad \text{and} \quad V = \begin{bmatrix} \gamma + \mu + a & 0 \\ -\xi & \delta + w \end{bmatrix}.$$

The basic reproductive number is then determined as the spectral radius of FV^{-1}, which yields

$$\mathcal{R}_0^c = \frac{\mu N}{(\delta + w)\kappa(\mu + v)(\gamma + \mu + a)} \left[\xi\beta_e + (\delta + w)\kappa\beta_h \right], \tag{9}$$

where we have used the superscript c to emphasize the model with controls. Compared to the basic reproductive number for the original no-control model [**16**],

$$\mathcal{R}_0 = \frac{N}{\delta\kappa(\gamma+\mu)}\big[\xi\beta_e + \delta\kappa\beta_h\big], \tag{10}$$

we can clearly see $\mathcal{R}_0^c \leq \mathcal{R}_0$. The result in equation (9) shows that, mathematically, each of the three types of individual controls can reduce the value of R_0^c lower than 1 so that the disease will be eradicated (unless backward bifurcation occurs, but we will show in Section 3.2 that this is not applicable to our model). For example, suppose $a = w = 0$; i.e., vaccination is the only control strategy implemented. Based on equation (9), we can readily see that if $\mathcal{R}_0 > 1$, there is a critical value for the vaccination strength, say v_0, such that

$$\frac{\mu N}{\delta\kappa(\mu+v_0)(\gamma+\mu)}\big[\xi\beta_e + \delta\kappa\beta_h\big] = 1\,,$$

or

$$v_0 = \frac{\mu N}{\delta\kappa(\gamma+\mu)}\big[\xi\beta_e + \delta\kappa\beta_h\big] - \mu\,. \tag{11}$$

When $v > v_0$, $\mathcal{R}_0^c < 1$ and the disease can be eradicated. In contrast, when $v < v_0$, $\mathcal{R}_0^c > 1$ and the disease will persist. Practically, however, the strength of each control strategy would be limited by social and economic factors as well as available resources, and the combination of different intervention approaches would possibly achieve the best result. We will further explore this point in the optimal control study in Section 4.

It follows from Theorem 2 in [**25**], that the disease-free equilibrium is locally asymptotically stable when $\mathcal{R}_0^c < 1$. In contrast, if the controls are not strong enough such that $\mathcal{R}_0^c > 1$, then the DFE becomes unstable and a disease outbreak occurs. Let us compare the outbreak growth rates between the original model and the model with controls. The positive (dominant) eigenvalue of the Jacobian matrix at the DFE characterizes the initial outbreak growth rate [**24**]. For the system (5–7), the Jacobian at the DFE is given by

$$J(\mathcal{E}_0) = \begin{bmatrix} -(\mu+v) & -\frac{\mu\beta_h N}{\mu+v} & -\frac{\mu\beta_e N}{\kappa(\mu+v)} \\ 0 & \frac{\mu\beta_h N}{\mu+v} - (\gamma+\mu+a) & \frac{\mu\beta_e N}{\kappa(\mu+v)} \\ 0 & \xi & -(\delta+w) \end{bmatrix}.$$

The characteristic equation is

$$(12)\quad (\lambda+\mu+v)\Big[\lambda^2+(\gamma+\mu+a+\delta+w-\beta_h S_0)\,\lambda + (\delta+w)(\gamma+\mu+a-\beta_h S_0)-\frac{\xi\beta_e}{\kappa}S_0\Big]=0,$$

where $S_0=\frac{\mu N}{\mu+v}$. We can easily observe from equation (12) that there are two negative eigenvalues and one positive eigenvalue when $\mathcal{R}_0^c>1$; this positive eigenvalue is given by

$$(13)\quad \lambda_+^c=\frac{1}{2}\Big[\sqrt{(\gamma+\mu+a-\delta-w-\beta_h S_0)^2+\frac{4\xi\beta_e}{\kappa}S_0} - (\gamma+\mu+a+\delta+w-\beta_h S_0)\Big].$$

Graphically, the value of λ_+^c represents the steepness of the ascending infection curve (with respect to time) when $\mathcal{R}_0^c>1$. Thus, a higher λ_+^c indicates a more severe disease outbreak.

It is clear that $\lambda_+^c>0$ when $\mathcal{R}_0^c>1$, and $\lambda_+^c<0$ when $\mathcal{R}_0^c<1$. This result can also be interpreted by the values of the controls. For example, let us assume $\mathcal{R}_0>1$. If we set $a=w=0$ in equation (13), we see that when $v=0$, $\lambda_+^c>0$ (noting that $\mathcal{R}_0^c=\mathcal{R}_0>1$); and when v is large, $\lambda_+^c<0$ (noting that $\mathcal{R}_0^c<1$). Hence, there is a positive value for v, say v_0, such that $\lambda_+^c=0$; i.e.,

$$(14)\qquad \sqrt{(\gamma+\mu-\delta-\beta_h S_0)^2+\frac{4\xi\beta_e}{\kappa}S_0}=\gamma+\mu+\delta-\beta_h S_0.$$

Equation (14) yields the same expression for v_0 as given in (11). This provides another perspective on the critical value v_0, which is the vaccination strength that makes the initial outbreak growth rate exactly zero. Furthermore, taking the derivative of λ_+^c with respect to v (with $a=w=0$) yields

$$\frac{d\lambda_+^c}{dv}=\frac{\lambda_+^c}{dS_0}\frac{dS_0}{dv}=\frac{-\mu N}{(\mu+v)^2}\left[\frac{1}{2}\frac{(\gamma+\mu-\delta-\beta_h S_0)(-\beta_h)+\frac{2\xi\beta_e}{\kappa}}{\sqrt{(\gamma+\mu-\delta-\beta_h S_0)^2+\frac{4\xi\beta_e}{\kappa}S_0}}+\beta_h\right]$$

$$<0$$

when $\mathcal{R}_0^c > 1$. This implies, as can be expected, that increasing the strength of vaccination will reduce the disease outbreak growth rate.

In a similar way, we find the only positive eigenvalue of $J(\mathcal{E}_0)$ for the original cholera model, when $\mathcal{R}_0 > 1$, is given by

$$\lambda_+ = \frac{1}{2}\left[\sqrt{(\gamma+\mu-\delta-\beta_h N)^2 + \frac{4\xi\beta_e}{\kappa}N} - (\gamma+\mu+\delta-\beta_h N)\right]. \tag{15}$$

Equation (15) can also be obtained by setting $v = a = w = 0$ in equation (13). The following result is a natural consequence of incorporating the control measures.

Theorem 1. *Assume $v \geq 0$, $a \geq 0$ and $w \geq 0$. Then we have $\lambda_+^c \leq \lambda_+$. Furthermore, $\lambda_+^c = \lambda_+$ if and only if $v = a = w = 0$.*

The proof follows from elementary algebraic manipulations, noting that

$$\gamma + \mu + a + \delta + w - \beta_h S_0 \geq \gamma + \mu + \delta - \beta_h N.$$

In addition, we note that the DFE (8) is actually globally asymptotically stable when $\mathcal{R}_0^c < 1$. This can be easily established based on the DFE global stability condition theorem introduced by Castillo-Chavez *et al.* [**4**], together with the fact that the DFE is locally asymptotically stable when $\mathcal{R}_0^c < 1$.

We state the theorem below to summarize the above results:

Theorem 2. *When $\mathcal{R}_0^c < 1$, where R_0^c is defined in equation* (9)*, the DFE of the system* (5-7) *is both locally and globally asymptotically stable. When $\mathcal{R}_0^c > 1$, the DFE of the control model* (5–7) *is unstable, with a lower outbreak growth rate than that of the original no-control model.*

3.2 Endemic dynamics As mentioned before, when the effects of the controls are not strong enough to reduce R_0^c below 1 , the DFE becomes unstable and the disease will persist. Let us now study the endemic equilibrium for the long-term behavior of cholera dynamics.

Denote the endemic equilibrium of the model (5-7) by

$$\mathcal{E}^* = (S^*,\, I^*,\, B^*).$$

We first show the following result.

Theorem 3. *A unique positive endemic equilibrium exists for the system* (5–7) *if and only if* $\mathcal{R}_0^c > 1$.

Proof. From equations (5) and (7) we obtain

$$B^* = \frac{\xi I^*}{\delta + w} \qquad \text{and} \qquad S^* = \frac{\mu N}{\mu + v} - \frac{(\gamma + \mu + a) I^*}{\mu + v} .$$

Substituting these into the right-hand side of equation (6), we can derive a quadratic equation for I^* (after dropping the trivial solution $I^* = 0$):

$$A_1 I^{*2} + B_1 I^* + C_1 = 0 , \tag{16}$$

with

$$\begin{aligned} A_1 &= -\beta_h(\gamma + \mu + a)\xi, \\ B_1 &= \beta_h \xi \mu N - (\gamma + \mu + a)\big[\beta_e \xi + \beta_h(\delta + w)\kappa + (\mu + v)\xi\big], \\ C_1 &= \beta_e \xi \mu N - (\gamma + \mu + a)(\mu + v)(\delta + w)\kappa + \beta_h \mu \kappa N(\delta + w). \end{aligned}$$

The roots of this quadratic equation must satisfy,

$$I_1^* I_2^* = \frac{C_1}{A_1} \qquad \text{and} \qquad I_1^* + I_2^* = -\frac{B_1}{A_1} . \tag{17}$$

Note that $A_1 < 0$ always holds. If $\mathcal{R}_0^c > 1$, then $C_1 > 0$, and $I_1^* I_2^* = C_1/A_1 < 0$. Thus, equation (16) has a unique positive root I^* in this case. Consequently, B^* and S^* are uniquely determined and positive, as can be easily seen from the right-hand sides of equations (6) and (7). In contrast, if $\mathcal{R}_0^c < 1$, then $C_1 < 0$ so that $I_1^* I_2^* > 0$; if $\mathcal{R}_0^c = 1$, then $C_1 = 0$, and so $I_1^* I_2^* = 0$. Meanwhile, when $\mathcal{R}_0^c \le 1$, we have $\frac{\mu\beta_h N}{(\gamma+\mu+a)(\mu+v)} < 1$, or $\mu\beta_h\xi N < (\gamma+\mu+a)(\mu+v)\xi$; thus $B_1 < 0$, and $I_1^* + I_2^* = -B_1/A_1 < 0$. It then follows that when $\mathcal{R}_0^c < 1$, equation (16) has two negative roots which are biologically nonfeasible; when $\mathcal{R}_0^c = 1$, equation (16) has one zero root and one (biologically nonfeasible) negative root. □

Next we establish the following theorem.

Theorem 4. *When* $\mathcal{R}_0^c > 1$*, the endemic equilibrium* $\mathcal{E}^*$ *is locally asymptotically stable.*

Proof. The Jacobian of the system (5–7) at $\mathcal{E}^*$ is given by

$$J(\mathcal{E}^*) = \begin{bmatrix} -P-(\mu+v) & -\beta_h S^* & -Q \\ P & \beta_h S^* - (\gamma+\mu+a) & Q \\ 0 & \xi & -(\delta+w) \end{bmatrix},$$

where

$$P = \frac{\beta_e B^*}{\kappa + B^*} + \beta_h I^* \qquad \text{and} \qquad Q = \frac{\beta_e \kappa S^*}{(\kappa + B^*)^2}.$$

The characteristic polynomial of the matrix $J(\mathcal{E}^*)$ is

$$\det\left[\lambda I - J(\mathcal{E}^*)\right] = a_0\lambda^3 + a_1\lambda^2 + a_2\lambda + a_3, \tag{18}$$

where

$$\begin{aligned} a_0 &= 1, \\ a_1 &= P + (\delta+w) + (\mu+v) + \big(\gamma+\mu+a-\beta_h S^*\big), \\ a_2 &= \big[(\delta+w)(\gamma+\mu+a) - Q\xi - \beta_h S^*(\delta+w)\big] \\ &\quad + (\mu+v)\big(\gamma+\mu+a-\beta_h S^*\big) \\ &\quad + (P+\mu+v)(\delta+w) + P(\gamma+\mu+a), \\ a_3 &= (\mu+v)\big[(\delta+w)(\gamma+\mu+a) - Q\xi - \beta_h S^*(\delta+w)\big] \\ &\quad + P(\gamma+\mu+a)(\delta+w). \end{aligned}$$

The Routh-Hurwitz criterion [**19**] requires

$$a_1 > 0, \quad a_2 > 0, \quad a_3 > 0, \quad \text{and} \quad a_1 a_2 - a_0 a_3 > 0 \tag{19}$$

as the necessary and sufficient conditions for the locally asymptotical stability; i.e., all roots of the polynomial (18) have negative real parts. Note that at the endemic equilibrium, the right-hand sides of equations (6) and (7) become 0, which yields

$$\gamma + \mu + a = \beta_h S^* + \frac{\beta_e \xi S^*}{\kappa(\delta+w) + \xi I^*}. \tag{20}$$

From equation (20) we can easily obtain

$$\begin{aligned} \gamma + \mu + a - \beta_h S^* &> 0, \\ (\delta+w)(\gamma+\mu+a) - Q\xi - \beta_h S^*(\delta+w) &> 0. \end{aligned}$$

Using the fact that all model parameters as well as P and Q are positive, it is then straightforward to observe that all the inequalities in (19) hold. □

Combining Theorems 2, 3 and 4, we see that a forward transcritical bifurcation occurs at the bifurcation point $\mathcal{R}_0^c = 1$. Thus, the possibility of backward bifurcation is precluded in our model. This has important implication on the prevention and intervention strategies for cholera, as reducing the basic reproductive number below one by using single or multiple control measures would be sufficient to eradicate the disease.

4 Optimal control study Now we turn to the more general model (1–3) with time-dependent controls $v(t)$, $a(t)$ and $w(t)$. We consider the system on a time interval $[0, T]$. The functions $v(t)$, $a(t)$ and $w(t)$ are assumed to be at least Lebesgue measurable on $[0, T]$. The control set is defined as

$$\Omega = \big\{ \big(v(t),\, a(t),\, w(t)\big) \,\big|\, 0 \le v(t) \le v_{\max}\,, \quad 0 \le a(t) \le a_{\max}\,,\ 0 \le w(t) \le w_{\max} \big\},$$

where $v_{\max}$, $a_{\max}$ and $w_{\max}$ denote the upper bounds for the effort of vaccination, treatment, and sanitation. These bounds reflect practical limitations on the maximum rates of controls in a given time period.

The presence of time-dependent controls makes the analysis of the system (1–3) difficult. In fact, the disease dynamics now depend on the evolution of each control profile. In what follows we perform an optimal control study on this problem. We aim to minimize the total number of infections and the costs of controls over the time interval $[0, T]$; i.e.,

$$\min_{(v,a,w)\in\Omega} \int_0^T \big[I(t) + c_{21} v(t) S(t) + c_{22} v(t)^2 + c_{31} a(t) I(t) + c_{32} a(t)^2 + c_{41} w(t) + c_{42} w(t)^2 \big]\, dt. \tag{21}$$

Here, the parameters c_{ij} $(i = 2, 3, 4;\ j = 1, 2)$, with appropriate units, define the appropriate costs associated with these controls. Quadratic terms are introduced to indicate nonlinear costs potentially arising at high intervention levels [**2, 3, 17**]. Particularly, the cost terms associated with the sanitation, $c_{41} w(t) + c_{42} w(t)^2$, are taken from [**17**]. The minimization process is subject to the differential equations (1–3), which are

now referred to as the state equations. Correspondingly, the unknowns S, I and B are now called the *state variables*, in contrast to the *control variables* v, a and w. Our goal is to determine the optimal control, $v^*(t)$, $a^*(t)$ and $w^*(t)$, so as to minimize the objective functional in (21).

We first establish the following theorem on the existence of optimal control.

Theorem 5. *There exists* $\big(v^*(t),\, a^*(t),\, w^*(t)\big) \in \Omega$ *such that the objective functional in* (21) *is minimized.*

Proof. Note that the control set Ω is closed and convex, and the integrand of the objective functional in (21) is convex. Hence, based on the standard optimal control theorems in [**8**], the conditions for the existence of optimal control are satisfied, as our model is linear in the control variables. Indeed, the optimal control is also unique for small T due to the Lipschitz structure of the state equations and the boundedness of the state variables [**8, 12**]. □

We will follow the method described in [**2, 13**] to seek the optimal control solution. This method is based on Pontryagin's Maximum Principle [**20**] which introduces the adjoint functions and represents an optimal control in terms of the state and adjoint functions. Essentially, this approach transfers the problem of minimizing the objective functional (under the constraint of the state equations) into minimizing the Hamiltonian with respect to the controls.

Let us first define the adjoint functions λ_S, λ_I and λ_B associated with the state equations for S, I and B, respectively. We then form the Hamiltonian, H, by multiplying each adjoint function with the right-hand side of its corresponding state equation, and adding each of these products to the integrand of the objective functional. As a result, we obtain

$$\begin{aligned} H = {} & I(t) + c_{21}v(t)S(t) + c_{22}v(t)^2 + c_{31}a(t)I(t) \\ & + c_{32}a(t)^2 + c_{41}w(t) + c_{42}w(t)^2 \\ & + \lambda_S\big[\mu N - \beta_e S\frac{B}{\kappa + B} - \beta_h SI - \mu S - v(t)S\big] \\ & + \lambda_I\big[\beta_e S\frac{B}{\kappa + B} + \beta_h SI - (\gamma + \mu)I - a(t)I\big] \\ & + \lambda_B\big[\xi I - \delta B - w(t)B\big]. \end{aligned}$$

To achieve the optimal control, the adjoint functions must satisfy

$$\frac{d\lambda_S}{dt} = -\frac{\partial H}{\partial S} = -c_{21}v(t) + \lambda_S\left[\beta_e\frac{B}{\kappa+B} + \beta_h I + \mu + v(t)\right] - \lambda_I\big[\beta_e\frac{B}{\kappa+B} + \beta_h I\big], \tag{22}$$

$$\frac{d\lambda_I}{dt} = -\frac{\partial H}{\partial I} = -1 - c_{31}a(t) + \lambda_S\beta_h S - \lambda_I\big[\beta_h S - (\gamma+\mu) - a(t)\big] - \lambda_B\xi, \tag{23}$$

$$\frac{d\lambda_B}{dt} = -\frac{\partial H}{\partial B} = \lambda_S\beta_e\frac{\kappa S}{(\kappa+B)^2} - \lambda_I\beta_e\frac{\kappa S}{(\kappa+B)^2} + \lambda_B\big[\delta + w(t)\big], \tag{24}$$

with transversality conditions (or final time conditions):

$$\lambda_S(T) = 0, \qquad \lambda_I(T) = 0, \qquad \lambda_B(T) = 0. \tag{25}$$

The characterizations of the optimal controls, $v^*(t)$, $a^*(t)$ and $w^*(t)$, are based on the conditions

$$\frac{\partial H}{\partial v} = 0, \qquad \frac{\partial H}{\partial a} = 0, \qquad \frac{\partial H}{\partial w} = 0, \tag{26}$$

respectively, subject to the constraints $0 \le v \le v_{\max}$, $0 \le a \le a_{\max}$, and $0 \le w \le w_{\max}$. Specifically, we have

$$v^*(t) = \max\big[0,\ \min\big(\tilde{v}(t),\ v_{\max}\big)\big], \tag{27}$$

$$a^*(t) = \max\big[0,\ \min\big(\tilde{a}(t),\ a_{\max}\big)\big], \tag{28}$$

$$w^*(t) = \max\big[0,\ \min\big(\tilde{w}(t),\ w_{\max}\big)\big], \tag{29}$$

where

$$\tilde{v}(t) = \big[(\lambda_S - c_{21})S(t)\big] \,/\, (2c_{22}), \tag{30}$$

$$\tilde{a}(t) = \big[(\lambda_I - c_{31})I(t)\big] \,/\, (2c_{32}), \tag{31}$$

$$\tilde{w}(t) = \big[\lambda_B B(t) - c_{41}\big] \,/\, (2c_{42}). \tag{32}$$

We summarize the above results by the theorem below:

Theorem 6. *Given an optimal control* $\big(v^*(t),\ a^*(t),\ w^*(t)\big)$ *and corresponding solutions to the state equations* (5–7)*, there exist adjoint variables satisfying the system* (22–25)*. Furthermore, the optimal control of the problem* (21) *is represented by* (27–29)*.*

The overall optimality system, which consists of the state equations with the initial conditions, the adjoint equations with the transversality conditions, and the optimal control characterization, has to be solved numerically. We apply the forward-backward sweep method [**13**] to solve the optimality system in an iterative manner. First, the state equations are solved forward in time by a fourth-order Runge-Kutta method, with an initial guess for the control variables. Next, the adjoint equations are solved backward in time using the solutions of the state equations. The control is then updated with the new values of the state and adjoint solutions, and the process is repeated until the solutions converge.

To carry out the numerical simulation, we list the values for the various transmission rates in the state equations (5–7) in Table 1. Particularly, we take the values of μ, β_e and β_h from Zimbabwean cholera data [**16**]; their values are thus specific to Zimbabwe and may be different for other cholera endemic places. Meanwhile, the cost parameters in (21) are assigned with appropriate values [**17**]. We also set the initial infection number $I(0) = 1000$ and the entire period of time $T = 100$ days.

Parameter	Symbol	Value	Source
Total population	N	10,000	
Natural human birth and death rate	μ	$(43.5\text{yr})^{-1}$	[**26**]
Concentration of *V. cholerae* in environment	κ	10^6 cells/ml	[**6**]
Rate of recovery from cholera	γ	$(5\,\text{day})^{-1}$	[**9**]
Rate of human contribution to *V. cholerae*	ξ	10 cells/ml-day	[**9**]
Death rate of vibrios in the environment	δ	$(30\,\text{day})^{-1}$	[**9**]
Ingestion rate from the environment	β_e	0.075/day	[**16**]
Ingestion rate through human-human interaction	β_h	0.00011/day	[**16**]

TABLE 1: Cholera model parameters and values.

We first consider the following set of values for the cost parameters

$$c_{21} = 2, \quad c_{22} = 10, \quad c_{31} = 10, \quad c_{32} = 10, \quad c_{41} = 10, \quad c_{42} = 20. \tag{33}$$

The per capita cost for vaccination, c_{21} , takes a lower value than other costs, based on the fact that vaccination is usually the most commonly used intervention strategy for various infectious diseases. In particular,

the World Health Organization [**26**] has recently strengthened its recommendation for using oral cholera vaccines to control epidemic and endemic cholera.

Figure 1 shows the infection curves for the model without controls (dashed line), i.e., $v = a = w = 0$, and that with the optimal controls (solid line). It is clearly seen that the infection level has been significantly reduced due to the incorporation of the three types of controls. For comparison, let us also consider the case with vaccination being the only control measure. The optimal control problem can be reformulated to determine the optimal strategy for vaccination, by simply setting the other two controls to zero (i.e., $a = w = 0$) and using the same cost parameters for vaccination. The infection curve with this vaccination-only strategy is also shown in Figure 1 (dash-dot line). As can be expected, the infection level with vaccination only is slightly higher than that with multiple controls, yet it still shows significant improvement compared to the no-control infection curve.

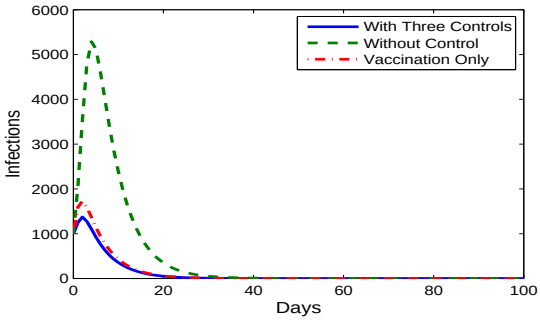

FIGURE 1: Infection curves for the cholera model without control ($v = a = w = 0$), with three controls in optimal balance, and with vaccination only ($a = w = 0$) in optimal setting, based on the cost parameters in (33).

Figure 2 shows the profiles of the optimal vaccination rates in these two cases, i.e., with three controls combined and with vaccination only. We observe a common pattern that the optimal vaccination rates are at the maximum ($u_{\max} = 0.7$) initially and remain at that level for several days (about 7 days for the first case, and 9 days for the second case), before decreasing to almost zero. The shorter period that the maximum vaccination rate stays in the first case is due to the combination of the

other two types of controls. Additionally, we sketch the profiles of the optimal treatment rate and sanitation rate in Figure 3. We observe that the therapeutic treatment starts with the maximum rate ($v_{\max} = 0.5$) but rapidly decays to a level close to zero, whereas the sanitation rate remains at a relatively low level for a much longer period of time.

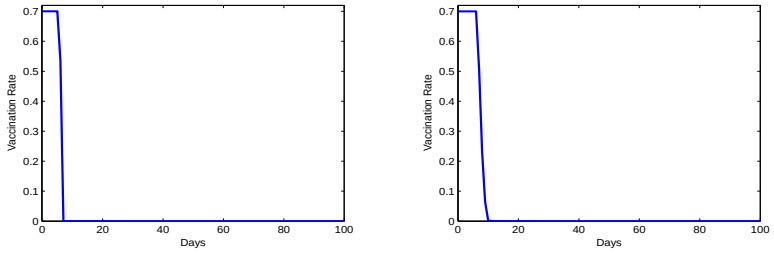

(a) (b)

FIGURE 2: Optimal vaccination rates for the two cases: (a) with three controls; and (b) vaccination only, based on the cost parameters in (33).

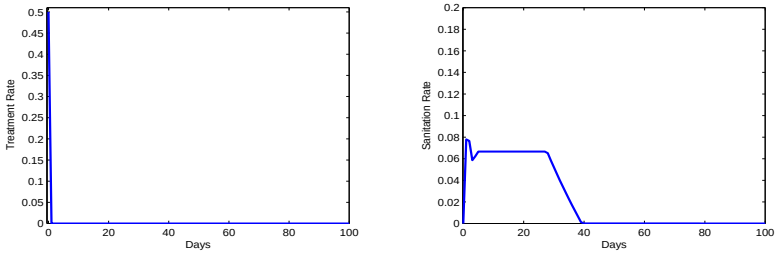

(a) (b)

FIGURE 3: Optimal balance of the treatment rate (a) and sanitation rate (b), based on the cost parameters in (33).

Next, we consider another set of values for the cost parameters, by decreasing the per capita cost for the therapeutic treatment and increasing the cost for sanitation:

$$c_{21} = 2, \quad c_{22} = 10, \quad c_{31} = 2, \quad c_{32} = 10, \quad c_{41} = 100, \quad c_{42} = 20. \tag{34}$$

The vaccination cost is kept the same as before. We again conduct simulations for the optimal strategy of the three controls combined and that for vaccination only. The results are presented in Figures 4–6.

With the reduced costs for therapeutic treatment, we observe that both the strength and effective period of the optimal vaccination rate are decreased (see Figure 5-a). On the other hand, the optimal treatment rate shows a significant increase (see Figure 6-a) to achieve the optimal balance between controls. The treatment rate starts with the maximum ($v_{\max} = 0.5$) and stays there for more than 20 days, then gradually decays but remains a significant level throughout almost the entire period of 100 days. The increased level of treatment also accounts for the rapid decay of the infection curve starting from the very beginning (see Figure 4, solid line). This observation indicates that there is an interaction between the vaccination and treatment in achieving the optimal balance; their relative costs play an important role in determining the length and strength of each control.

In addition, we see there is no significant change to the level of the optimal sanitation rates based on the two different sets of cost parameters (see Figure 3-b and Figure 6-b), which implies that the role of water sanitation in containing a cholera outbreak seems to be minor in the optimal balance of controls, under our model and population settings. Particularly, we note that our model parameters are specific to Zimbabwe, a land-locked country in middle Africa where the level of contact between infected people and the estuarine environment is relatively low.

Finally, we mention that similar patterns are observed for different initial infection sizes and different values of cost parameters, and other results are not shown here.

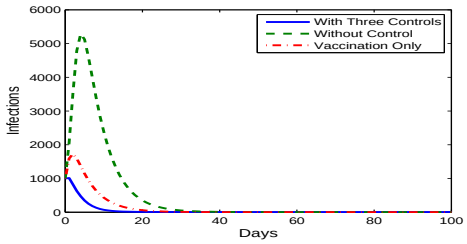

FIGURE 4: Infection curves for the cholera model without control ($v = a = w = 0$), with three controls in optimal balance, and with vaccination only ($a = w = 0$) in optimal setting, based on the cost parameters in (34).

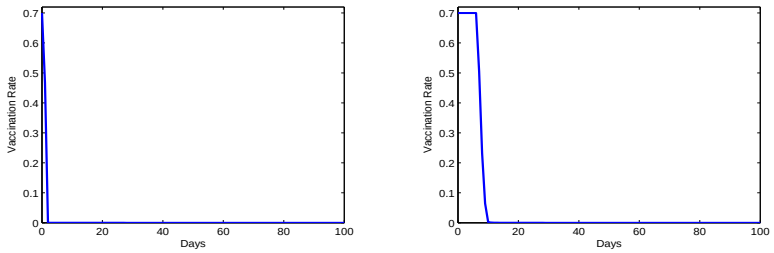

(a) (b)

FIGURE 5: Optimal vaccination rates for the two cases: (a) with three controls; and (b) vaccination only, based on the cost parameters in (34).

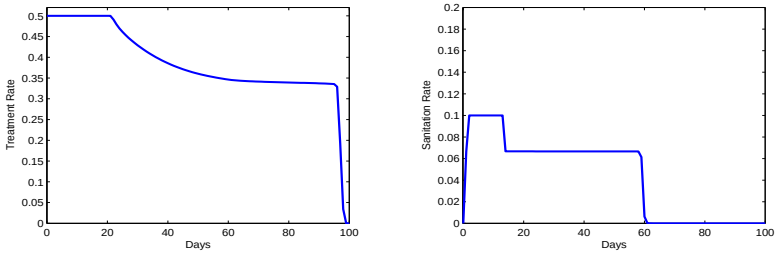

(a) (b)

FIGURE 6: Optimal balance of the treatment rate (a) and sanitation rate (b), based on the cost parameters in (34).

5 Conclusions We have presented a cholera epidemiological model by incorporating three types of intervention strategies: vaccination, therapeutic treatment, and water sanitation. This model represents a coupling between multiple transmission pathways of cholera and multiple control measures. In the case with constant controls, our equilibrium analysis shows that the basic reproductive number for the control model, R_0^c, plays a crucial role in determining the epidemic and endemic dynamics. Specifically, we have established $R_0^c = 1$ as a sharp threshold for stability exchange between the DFE and the endemic equilibrium. For

general time-dependent controls, we have applied the optimal control theory to explore cost-effective balance of multiple intervention strategies against cholera outbreaks. Out simulation results show that different controls (such as vaccination and treatment) closely interplay with each other, and the specific population settings and relative costs determine the length and strength of each control in an optimal strategy. We have found that a combination of multiple intervention methods generally achieves better results than a single control such as vaccination only.

Acknowledgment JW acknowledges partial support from the National Science Foundation (under Grant No. DMS-0813691). This work was also partially supported by a grant from the Simons Foundation (No. 208716 to JW). The authors thank the anonymous referee for the helpful comments to improve this paper.

REFERENCES

1. A. Alam, R. C. Larocque, J. B. Harris *et al.*, *Hyperinfectivity of human-passaged Vibrio cholerae can be modeled by growth in the infant mouse,* Infection Immunity **73** (2005), 6674–6679.
2. E. Asano, L. J. Gross, S. Lenhart and L. A. Real, *Optimal control of vaccine distribution in a rabies metapopulation model*, Math. Biosci. Eng. **5** (2008), 219–238.
3. B. Buonomo, *A simple analysis of vaccination strategies for Rubella,* Math. Biosci. Eng. **8** (2011), 677–687.
4. C. Castillo-Chavez, Z. Feng and W. Huang, *On the computation of R_0 and its role on global stability*, in Mathematical approaches for emerging and reemerging infectious diseases: an introduction (C. Castillo-Chavez *et al.*, eds.), IMA **125** (2002), 229–250.
5. Center for Disease Control and Prevention web page: www.cdc.gov.
6. C. T. Codeço, *Endemic and epidemic dynamics of cholera: the role of the aquatic reservoir*, BMC Infectious Diseases **1** (2001), 1.
7. G. W. Cross, *Three types of matrix stability,* Linear Algebra Appl. **20** (1978), 253–263.
8. W. H. Fleming and R. W. Rishel, *Deterministic and Stochastic Optimal Control*, Springer, New York, 1975.
9. D. M. Hartley, J. G. Morris Jr. and D. L. Smith, *Hyperinfectivity: A critical element in the ability of* V. cholerae *to cause epidemics?* PLoS Medicine **3** (2006), 0063–0069.
10. B. S. Gou, *Global stability in two species interactions,* J. Math. Biol. **3** (1976), 313–318.
11. R. I. Joh, H. Wang, H. Weiss and J. S. Weitz, *Dynamics of indirectly transmitted infectious diseases with immunological threshold,* Bull. Math. Biol. **71** (2009), 845–862.

12. E. Jung, S. Iwami, Y. Takeuchi and T.-C Jo, *Optimal control strategy for prevention of avian influenza pandemic*, J.Theor. Biol. **260** (2009), 220–229.
13. S. Lenhart and J. Workman, *Optimal Control Applied to Biological Models*, Chapman Hall/CRC, 2007.
14. S. Liao and J. Wang, *Stability analysis and application of a mathematical cholera model,* Math. Biosci. Eng. **8** (2011), 733–752.
15. D. S. Merrell, S. M. Butler, F. Qadri *et al.*, *Host-induced epidemic spread of the cholera bacterium,* Nature **417** (2002), 642–645.
16. Z. Mukandavire, S. Liao, J. Wang, H. Gaff, D. L. Smith and J. G. Morris Jr., *Estimating the reproductive numbers for the 2008-2009 cholera outbreaks in Zimbabwe*, Proc. Nat. Acad. Sci. **108** (2011), 8767–8772.
17. R. L. M. Neilan, E. Schaefer, H. Gaff, K. R. Fister and S. Lenhart, *Modeling optimal intervention strategies for cholera,* Bull. Math. Biol. **72** (2010), 2004–2018.
18. E. J. Nelson, J. B. Harris, J. G. Morris, S. B. Calderwood and A. Camilli, *Cholera transmission: the host, pathogen and bacteriophage dynamics*, Nature Rev.: Microbiology **7** (2009), 693–702.
19. R. M. Nisbet and W. S. C. Gurney, *Modeling Fluctuating Populations*, John Wiley & Sons, New York, 1982.
20. L. S. Pontryagin, V. G. Boltyanski, R. V. Gamkrelize and E. F. Mishchenko, *The Mathematical Theory of Optimal Processes*, Wiley, New York, 1967.
21. R. Redheffer, *Volterra multipliers I*, SIAM J. Algebraic Discrete Methods **6** (1985), 592–611.
22. R. Redheffer, *Volterra multipliers II*, SIAM J. Algebraic Discrete Methods **6** (1985), 612–623.
23. J. Tian and J. Wang, *Global stability for cholera epidemic models,* Math. Biosci. **232** (2011), 31–41.
24. J. H. Tien and D. J. D. Earn, *Multiple transmission pathways and disease dynamics in a waterborne pathogen model*, Bull. Math. Biol. **72** (2010), 1502–1533.
25. P. van den Driessche and J. Watmough, *Reproduction numbers and sub-threshold endemic equilibria for compartmental models of disease transmission,* Math. Biosci. **180** (2002), 29–48.
26. World Health Organization web page: www.who.org.

Department of Mathematics and Statistics,
Old Dominion University, Norfolk, VA 23529, USA
E-mail address: j3wang@odu.edu